

## Efficacy of cabazitaxel in mouse models of pediatric brain tumors

Emily Girard, Sally Ditzler, Donghoon Lee, Andrew Richards, Kevin Yagle, Joshua Park, Hedieh Eslamy, Dmitri Bobilev, Patricia Vrignaud, and James Olson

Clinical Research Division, Fred Hutchinson Cancer Research Center, Seattle, Washington (E.G., S.D., A.R., J.O.); Department of Radiology, University of Washington, Seattle, Washington (D.L., K.Y., J.P., H.E.); Sanofi Oncology, Global Oncology Division, Cambridge, Massachusetts 02142 (D.B.); Oncology/Translational and Experimental Medicine, Sanofi Inc, Vitry sur Seine, France (P.V.)

**Corresponding Author:** James Olson, PhD, 1100 Fairview Ave N, D4-100, Seattle, WA 98109 (jolson@fhcrc.org).

**Background.** There is an unmet need in the treatment of pediatric brain tumors for chemotherapy that is efficacious, avoids damage to the developing brain, and crosses the blood-brain barrier. These experiments evaluated the efficacy of cabazitaxel in mouse models of pediatric brain tumors.

**Methods.** The antitumor activity of cabazitaxel and docetaxel were compared in flank and orthotopic xenograft models of patient-derived atypical teratoid rhabdoid tumor (ATRT), medulloblastoma, and central nervous system primitive neuroectodermal tumor (CNS-PNET). Efficacy of cabazitaxel and docetaxel were also assessed in the Smo/Smo spontaneous mouse medulloblastoma tumor model.

**Results.** This study observed significant tumor growth inhibition in pediatric patient-derived flank xenograft tumor models of ATRT, medulloblastoma, and CNS-PNET after treatment with either cabazitaxel or docetaxel. Cabazitaxel, but not docetaxel, treatment resulted in sustained tumor growth inhibition in the ATRT and medulloblastoma flank xenograft models. Patient-derived orthotopic xenograft models of ATRT, medulloblastoma, and CNS-PNET showed significantly improved survival with treatment of cabazitaxel.

**Conclusion.** These data support further testing of cabazitaxel as a therapy for treating human pediatric brain tumors.

**Keywords:** animals/in vivo models for carcinogenesis, brain/central nervous system cancers, pediatric cancers.

Malignancies of the central nervous system are the most common type of solid tumor affecting children.<sup>1</sup> The outcome for children diagnosed with central nervous system tumors such as medulloblastoma has improved in recent years, largely due to aggressive surgical resection and craniospinal radiation.<sup>2,3</sup> Poor outcomes in young patients are often attributed to incomplete resection and the avoidance of radiation therapy due to concerns about neurocognitive toxicities.<sup>2</sup> Despite improvements in prolonged survival, the treatment of these tumors often results in significant long-term disabilities.<sup>4</sup> There is a great need for therapies with both fewer neurotoxic side effects and improved event-free survival in pediatric patients with central nervous system tumors.

The blood-brain barrier (BBB) presents a challenge in delivering therapeutics to tumors of the central nervous system. The capillary endothelial cells of the brain differ from endothelial cells of other tissues in that they lack fenestrations and are joined by tight junctions that prevent the passive diffusion of therapeutics into the brain.<sup>5,6</sup> Additionally, capillary endothelial cells express efflux transporters such as P-glycoprotein (Pgp),

which actively eliminate therapeutics that penetrate the luminal membrane.<sup>7</sup> This physiology creates a privileged environment in the brain that protects neurons from potential toxins. Approximately 98% of all small molecule therapeutics fail to penetrate the BBB.<sup>8</sup> Most small molecules that do cross the BBB do so at a fraction of their plasma concentration.<sup>9</sup>

Selectively penetrating the BBB is important when treating tumors that cannot be resected. It could also benefit very young patients, in which radiation therapy is avoided or delayed due to neural, endocrine, and cognitive disabilities that may result from craniospinal radiation.<sup>10</sup> Although bulky primary brain tumors often show disruption of the BBB, as evidenced by gadolinium contrast staining during MRI, cells at the leading edge of the infiltrating tumor and tumor cells remaining after surgery and radiation may be sequestered behind a restored BBB and become inaccessible to secondary treatments.<sup>11</sup>

Taxane therapies are widely used and effective in the treatment of adult solid tumors.<sup>12</sup> The first generation taxanes (paclitaxel and docetaxel) are not without limitations. Paclitaxel and docetaxel are high-affinity substrates for

Received 5 March 2014; accepted 9 July 2014

© The Author(s) 2014. Published by Oxford University Press on behalf of the Society for Neuro-Oncology. All rights reserved.

For permissions, please e-mail: journals.permissions@oup.com.

multidrug-resistant pumps, in particular the ATP-dependent Pgp pump.<sup>13</sup> The affinity of Pgp pumps to paclitaxel and docetaxel may direct the innate and acquired resistance to taxanes. The affinity of Pgp pumps for paclitaxel and docetaxel also prevents these compounds from penetrating the BBB because their rate of influx into endothelial cells is matched by their rate of efflux.<sup>13</sup> In the pediatric setting, paclitaxel and docetaxel have undergone preclinical evaluation in models of sarcoma and leukemia but have failed to progress beyond phase II clinical trials.<sup>14–16</sup>

Cabazitaxel is a second-generation taxane currently approved for the second-line treatment of docetaxel-resistant, castration-resistant prostate cancer.<sup>17</sup> Cabazitaxel has been shown to have favorable drug properties, similar to docetaxel, with a high total body clearance (53.5 L/h/m<sup>2</sup>), a large volume of distribution (2034 L/m<sup>2</sup>), and dose-limiting toxicity consisting primarily of neutropenia.<sup>12</sup> Cabazitaxel has been shown to be more active in Pgp-expressing cell lines compared with paclitaxel and docetaxel, due to a higher logP leading to better cell penetration.<sup>18</sup> In mouse models, the Pgp pump saturation threshold for cabazitaxel in normal brain tissue has been shown to be ~11  $\mu$ M.<sup>13</sup> Additionally, it has been shown that cabazitaxel is distributed throughout the brain parenchyma once it has been taken up by the endothelial cells of the BBB.<sup>13,18</sup> Though previous taxane therapies have not proven successful in pediatric or neuro-oncology, these characteristics may make cabazitaxel an effective therapeutic in this setting.

This study used 3 patient-derived xenograft models (atypical teratoid rhabdoid tumor [ATRT], medulloblastoma, and central nervous system primitive neuroectodermal tumor [CNS-PNET]) and a genetic mouse model of medulloblastoma to evaluate the relative efficacy of cabazitaxel and docetaxel in pediatric brain tumors. Median survival of mice bearing patient-derived tumor models of ATRT, medulloblastoma, and CNS-PNET were evaluated after treatment with each drug. Spontaneously arising tumors in the Smo/Smo mouse medulloblastoma model were evaluated for tumor burden in response to treatment with cabazitaxel or docetaxel in the presence of an intact BBB.

## Methods

All mice were maintained in accordance with the NIH Guide for the Care and Use of Experimental Animals with approval from the Fred Hutchinson Cancer Research Center Institutional Animal Care and Use Committee (IR#1457).

### Tumor Flank Allografts and Xenografts

For the generation of flank tumor allografts and xenografts, cells were harvested from symptomatic intracranial tumors in donor mice and dissociated into a single-cell suspension. Cell count and viability were determined using a Vi-Cell Cell Viability Analyzer (Beckman Coulter).  $3–5 \times 10^6$  cells suspended in phosphate-buffered saline with 50% Matrigel were implanted unilaterally into the flank of recipient mice. Smo/smo tumors were implanted into 6–8 week old C57BL6 male or female mice, and pediatric patient-derived tumors were hosted in 6–8 week old female athymic nude mice. All tumor cells were taken directly from one mouse to the next without culturing in a dish. Tumors were allowed to grow to 100–300 mm<sup>3</sup> before being assigned

to treatment groups, normalizing for tumor size. Mice were dosed by i.p. injection on days 1, 3, and 5. The therapeutic vehicle consisted of (v/v) 5% ethanol + 5% polysorbate-80 + 90% of an aqueous sucrose (5%) solution. Mouse weight and tumor dimensions were recorded 3 times per week until the tumor reached 2500 mm<sup>3</sup> or for 60 days. Tumors were measured with calipers, and volumes were extrapolated using the formula: tumor volume (mm<sup>3</sup>) = (length $\times$ width<sup>2</sup>)  $\times$  0.5. Tumor tissue was collected after euthanasia by CO<sub>2</sub> asphyxiation and preserved in 10% neutral buffered formalin.

### Dose Determination

The maximum tolerated dose (MTD) was determined for C57BL6 mice. Four C57BL6 mice bearing Smo/Smo flank allograft tumors were treated with 9, 15, or 25 mg/kg cabazitaxel or docetaxel IP on days 1, 3, and 5. Blood was collected by retro-orbital bleeding on days 8 and 15. Tumor volume was measured to determine the efficacious dose, and a complete blood chemistry panel (Phoenix Central Laboratory for Veterinarians) was conducted to evaluate symptoms of toxicity. The MTD for docetaxel and cabazitaxel in nude and severe combined immunodeficiency (SCID) background mice has been previously reported.<sup>18,19</sup>

### Orthotopic Brain Tumor Models

The Smo/Smo transgenic mice were generated and maintained on a C57BL6 background, as previously described.<sup>20,21</sup> Medulloblastoma tumors arise spontaneously in mice between 4 and 6 months of age. Male or female mice were enrolled into the study when they bore cerebellar tumors between 4 and 16 mm<sup>2</sup> and maintained an intact BBB. Both tumor volume and BBB integrity were determined by MRI. At the conclusion of MRI study initiation scans, 32 mice were found to have tumors eligible for study enrollment. Ten mice were randomly placed in the vehicle and docetaxel groups, and 12 mice were randomly placed in the cabazitaxel group. Mice were treated with 15 mg/kg cabazitaxel, docetaxel, or vehicle by i.p. injection on days 1, 3, and 5. Mouse weights were recorded 3 times a week for 9 weeks, and MRI was repeated 3, 5, and 9 weeks after treatment. Gadolinium contrast agent was included in scans conducted at enrollment, 5 weeks, and 9 weeks. Mice were removed from the study if they became moribund or 9 weeks after treatment.

Orthotopic pediatric patient-derived xenograft models were created by implanting  $1 \times 10^5$  tumor cells in suspension through a 1 mm bur hole in the right frontal region of the calvarium (or in the cerebellum for medulloblastoma), ~3 mm beneath the dura. Tumor cells came from symptomatic intracranial tumors in donor mice. Male and female NOD:scid gamma mice between 6 and 8 weeks of age were used in these experiments. The time between surgical implant of tumors and initiation of treatment was based on historic data of the typical time between surgery and development of symptomatic tumors for each model. Two weeks before symptomatic tumor burden was expected, 2 randomly chosen mice were given 100  $\mu$ L (20  $\mu$ M) i.v. injections of Cy5.5 conjugated chlorotoxin (CTX: Cy5.5 Tumor Paint [Blaze Bioscience]). Three hours after administration of CTX: Cy5.5, the mouse brains

were removed and imaged in the near-infrared spectrum, as previously described.<sup>22,23</sup> After verification of tumor burden in representative mice, the remaining animals were randomly placed into treatment groups. Mice were dosed with 15 mg/kg cabazitaxel or docetaxel on days 1 and 3 to achieve the MTD of 30 mg/kg in SCID background mice, which has been previously reported and shown to be efficacious in other preclinical tumor models.<sup>18,19</sup> Published studies on the pharmacokinetics of cabazitaxel and its accumulation in the brain suggest that cabazitaxel is more likely to saturate the Pgp efflux threshold and penetrate the BBB when given less frequently at a higher dose (twice at 15 mg/kg) than more prolonged dosing (3 times at 10 mg/kg).<sup>12,13</sup> Body weight was recorded 3 times per week for 60 days or until the mouse became moribund.

### Magnetic Resonance Imaging

High resolution MRI was performed on a 14T Avance 600 MHz/89 mm wide-bore vertical MR spectrometer (Bruker BioSpin) using a 25 mm inner diameter <sup>1</sup>H birdcage radiofrequency (RF) coil (Bruker BioSpin). The 14T MR system was equipped with actively shielded gradient coils (maximum gradient strength of 100 G/cm) and a Paravision (version 5.1) console interface.

A rapid acquisition with refocused echoes sequence was used to acquire 2-dimensional (2D) multislice images covering the entire mouse. Respiration was monitored throughout the MRI acquisition using a pressure sensor located on the back of a mouse (SA Instrument). To examine the BBB, baseline pre-contrast imaging was conducted by obtaining 5 T1-weighted images prior to i.p. gadolinium DTPA (Gd-DTPA) injection (0.1 mM/kg gadopentetate dimeglumine; 3-4 × dilute; Magnevist; Berlex Laboratories). Injection volume for the i.p. administration was ~500 µL for each mouse to achieve a dose of 2–2.5 mM/kg. Immediately after the Gd-DTPA injection, T1-weighted images were serially acquired over 12 minutes. T2-weighted images were used to identify tumor from normal brain tissue. Multislice 2D images covering the brain were reconstructed to create a 3-dimensional image using Amira software (version 5.4, Visualization Sciences Group). To calculate tumor volume, hyperintense tumor regions were segmented from the 2D imaging slices covering a tumor. The areas of each segmented tumor region were added and multiplied by the slice thickness to compute the tumor volume. Volumes of both the entire brain and tumor were calculated to monitor tumor growth and enlargement of ventricles.

### Statistical Analysis

Statistical analysis for changes in tumor volume and mouse survival consisted of ANOVA (survival) or RM-ANOVA (tumor volume) with Bonferroni test for significance.

## Results

### Determination of the Maximum Tolerated Dose for C57BL6 Mice

This study treated medulloblastoma allograft-bearing C57BL6 mice with 9, 15, or 25 mg/kg cabazitaxel or docetaxel to

establish the MTD. Mice experienced weight loss with both treatments at all 3 dosing levels, the greatest average weight loss being  $6.62\% \pm 4.54\%$  as shown in Fig. 1. The 25 mg/kg dosing groups exhibited the greatest and most sustained average weight loss of  $8\% \pm 3.56\%$  for docetaxel and  $4.75\% \pm 3.30\%$  for cabazitaxel. All mice recovered from the weight loss and returned to their starting weight by day 20. One mouse from both of the 25 mg/kg treatment groups died on day 8 of the study. Complete blood counts (CBC) on day 8 indicated that mice experienced transient thrombocytosis with normal blood counts restored by day 15 (Fig. 1). The CBC panel also indicated that mice may have experienced neutropenia on day 8 from treatment with cabazitaxel or docetaxel, but there was not sufficient statistical power to make the observation significant. Based on the observed deaths in the 25 mg/kg treatments, 15 mg/kg was selected as the dose for subsequent studies in mice with the C57BL6 background. This dosing scheme of 15 mg/kg on days 1, 3, and 5 is similar, though not identical, to what has been reported as efficacious in other mouse tumor models.<sup>18,19</sup>

### Cabazitaxel Causes Regression of Flank Tumors

Flank allograft and xenograft tumors were treated with cabazitaxel or docetaxel and evaluated by caliper measurement to determine the relative efficacy of the 2 therapeutics in the absence of the BBB. The Smo/Smo mouse medulloblastoma allografts showed a partial response in tumor growth at 15 mg/kg, as illustrated in Fig. 1. Three of 4 cabazitaxel-treated tumors regressed to the point of no palpable tumor; one of 4 was not impacted by the treatment. All 5 docetaxel-treated tumors showed no change on tumor growth as compared with the vehicle-treated mice. Tumor regression was not observed in any of the tumors treated with 9 mg/kg cabazitaxel or docetaxel.

All 3 pediatric patient-derived tumor flank xenograft models responded to cabazitaxel treatment (Fig. 2). In each of the 3 models, cabazitaxel and docetaxel both showed significant tumor growth inhibition, between 75% and 95%, when compared with vehicle at the time the vehicle group reached the maximum allowable tumor volume (2500 mm<sup>3</sup>). At this time point (day 36 for ATRT-310FH, day 22 for MED-211FH, and day 32 for PNET-109FH), the tumor volume was not significantly different between the cabazitaxel and docetaxel groups. Cabazitaxel and docetaxel treatment groups were allowed to continue growing after removal of the vehicle groups until the maximum allowable tumor volume was reached or to day 60. In both the ATRT-310FH and MED-211FH flank xenograft models (Fig. 2A and B), the cabazitaxel and docetaxel groups were significantly different from the vehicle, but not from each other ( $P < .001$ ), at the time the vehicle group was removed from the study. The Med-211FH model continued to day 33 when the docetaxel-treated group reached the maximum allowable tumor volume. On day 33, the tumors of the cabazitaxel-treated mice were significantly smaller than those of the docetaxel-treated mice ( $P < .0001$ ). When the ATRT-310FH study was terminated on day 60, cabazitaxel-treated tumors were significantly smaller than those of the docetaxel group ( $P < .0001$ ). No palpable tumor was observed after day 3

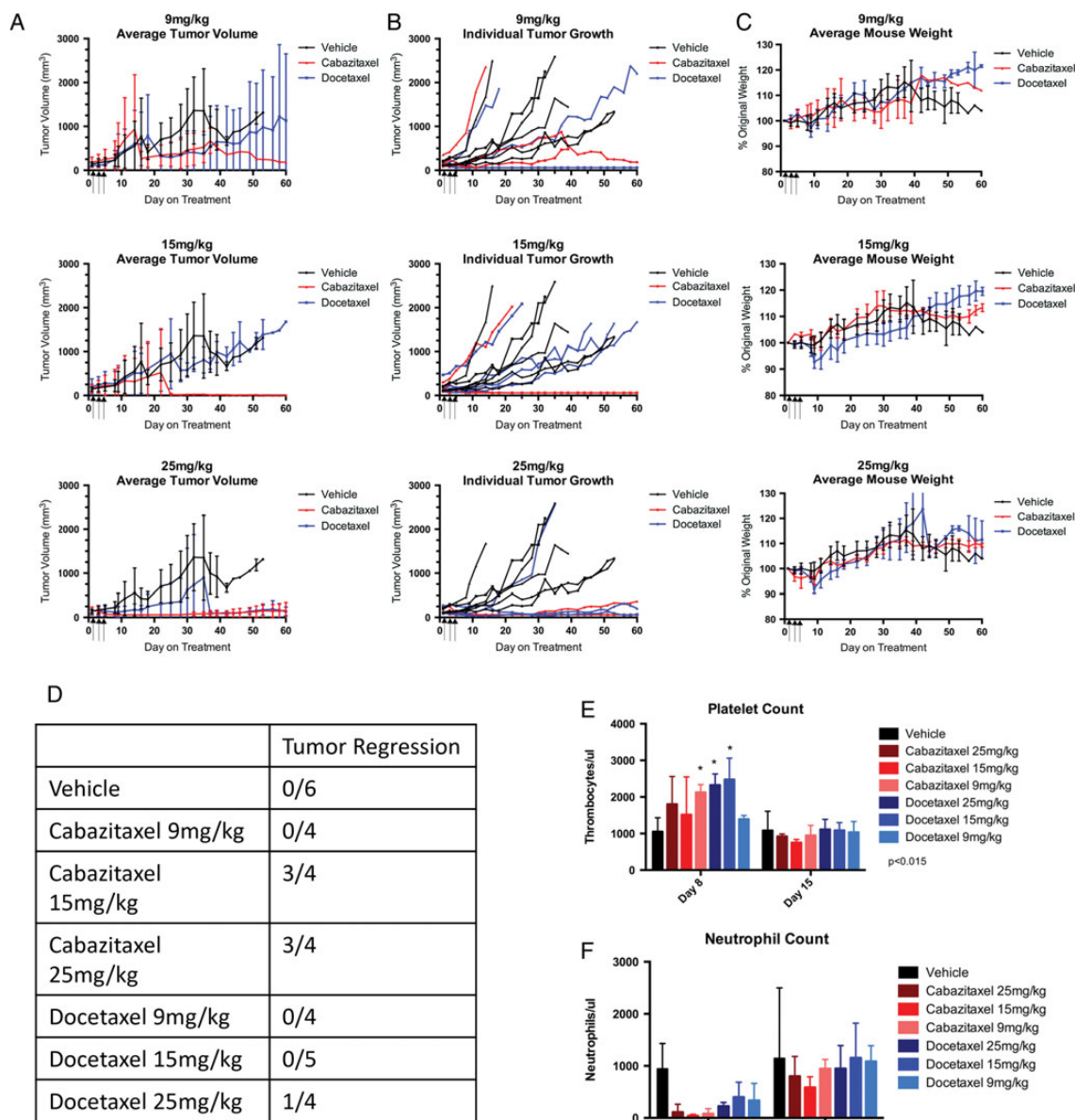


**Fig. 1.** Dose response of smo/smo flank tumor allografts in C57BL6 mice. Spontaneously arising hedgehog-driven Smo/Smo mouse medulloblastoma tumors were transplanted as flank allografts into C57BL6 mice. Mice were randomly placed into treatment groups when tumors measured 150–300 mm<sup>3</sup> and dosed with 9, 15, or 25 mg/kg on days 1, 3, and 5 after group placement ( $n = 4$ ). Blood was collected on days 8 and 15 for assessment of toxicity. (A) Mean tumor volume (mm<sup>3</sup>)  $\pm$  SEM for 9 mg/kg, 15 mg/kg, or 25 mg/kg dosing groups. (B) Tumor volume for individual mice in each dosing group. (C) Average mouse weight as a percent of the starting weight for each dosing group  $\pm$  SEM. (D) Tumor regression analysis of each dosing group. Tumor regression defined as a tumor that dropped below 60 mm<sup>3</sup> after exceeding 150 mm<sup>3</sup>. Blood was collected by retro-orbital bleed 8 days or 15 days after initiation of treatment. (E) Platelet count (mean  $\pm$  SEM) for each treatment and dosing group. (F) Neutrophil count (mean  $\pm$  SEM) for each treatment and dosing group.

(cabazitaxel) or day 5 (docetaxel) in any of the mice bearing the PNET-109FH tumor model (Fig. 2C).

### *Smo/Smo Brain Tumor Progression was Independent of Treatment*

The efficacy of cabazitaxel was tested against spontaneously arising, hedgehog-driven, Smo/Smo medulloblastoma.

Enrollment criteria for this study were tumor dimensions between 2 mm and 4 mm (tumor volume between 4 and 16 mm<sup>3</sup>). Mice were stratified into treatment groups to normalize for initial tumor volume, mouse age at enrollment, sex, and body weight. Ten mice were enrolled in each of the vehicle and docetaxel treatment groups, and 12 mice were enrolled in the cabazitaxel group. Four vehicle-, 5 docetaxel-, and 7 cabazitaxel-treated mice survived the 9-week study duration

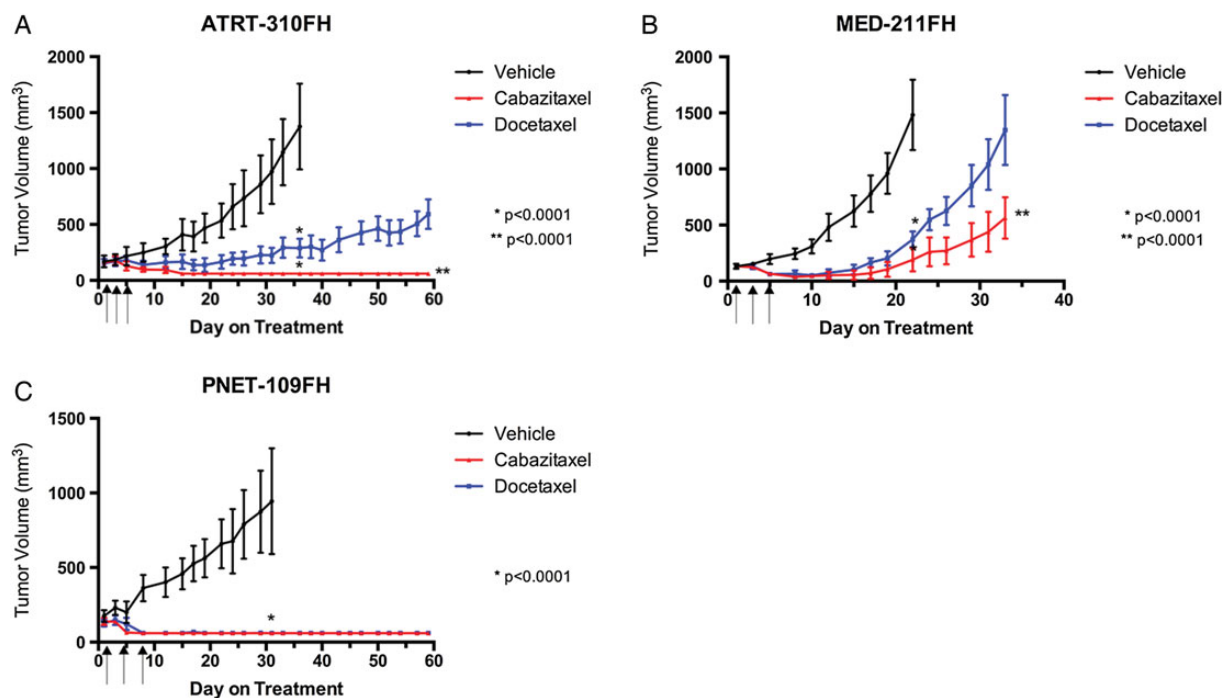


**Fig. 2.** Antitumor activity of cabazitaxel and docetaxel in pediatric patient-derived flank xenografts. Patient-derived models of ATRT, medulloblastoma, and CNS-PNET were transplanted as subcutaneous flank xenografts into female nude mice. Treatment groups were randomly assigned when tumors reached 150–300 mm<sup>3</sup>. Cabazitaxel or docetaxel were administered on days 1, 3, and 5 by i.p. injection at 15 mg/kg. Data are reported as mean tumor volume  $\pm$  SEM. Statistical analysis of tumor growth was performed comparing tumor volume of the vehicle with the cabazitaxel and docetaxel treatment groups at the time the vehicle group was removed due to tumor size. Cabazitaxel and docetaxel treatment groups were allowed to continue for 60 days or until the tumor volume limit was reached. Statistical analysis comparing cabazitaxel to docetaxel was performed at the termination of the study. (A) ATRT-310FH; (B) MED-211FH; (C) PNET-109FH.

without succumbing to tumor burden. The effect of treatment on tumor growth was considered in a number of ways including tumor volume, time of death, tumor volume in all mice that survived 3, 5, or 9 weeks, and change in volume from enrollment. No difference in tumor volume between treatment groups was observed at any time point (Fig. 3A). As in the treatment of flank xenografts, a pattern of weight loss during treatment, which resolved by day 20, was observed in mice receiving cabazitaxel or docetaxel (Fig. 3B). Hydrocephalus is an observed feature in this model and was noted in some mice, as evidenced by an increase in total brain volume that was attributed to an increase in ventricle size, but not tumor volume by MRI scan (data not shown). Neither cabazitaxel nor docetaxel treatment was observed to promote or protect from the development of hydrocephalus. The mice that succumbed to disease at 5 weeks, regardless of treatment group, had significantly greater brain volume (ie, hydrocephalus) than mice that survived to 9 weeks. No significant difference in survival was observed for either of the treatments within the 9-week study (Fig. 3C).

#### **The Blood-brain Barrier Is Maintained in the Majority of *Smo/Smo* Spontaneous Brain Tumors**

The integrity of the BBB was evaluated as a criterion for enrollment of the *Smo/Smo* spontaneous medulloblastoma mice into treatment groups. MR imaging with gadolinium contrast staining

at 5 and 9 weeks after treatment monitored the maintenance of the BBB throughout the study. Control regions in eye orbits and ears confirmed gadolinium uptake and lack of signal enhancement in the tumor-verified BBB integrity. At initial MR imaging, 35 mice bore tumors of the appropriate size for study enrollment. Three mice with acceptably sized tumors were excluded from the study due to gadolinium contrast staining that indicated a compromised BBB. Five of the 32 enrolled mice showed BBB disruption at the time they were removed from the study. Of the 5 mice exhibiting BBB disruption, 3 were observed at the 9-week MRI session, one from each group. One mouse from the vehicle group and one from the cabazitaxel group showed BBB disruption at 5 weeks and had to be removed from the study prematurely due to tumor burden. Twenty-seven mice completed the study without BBB disruption. The results of their MR scans were used to determine progression in tumor burden between the 3 treatment groups.

#### **Cabazitaxel Treatment Significantly Extends Survival of Mice With Orthotopic, Patient-derived Brain Tumor Xenografts**

The survival benefit of cabazitaxel or docetaxel treatment was tested in orthotopic pediatric patient-derived tumor xenografts. In all 3 models (ATRT-310FH, MED-211FH, and PNET-109FH), median survival was significantly improved with cabazitaxel treatment compared with vehicle (Fig. 4B). Mean survival of

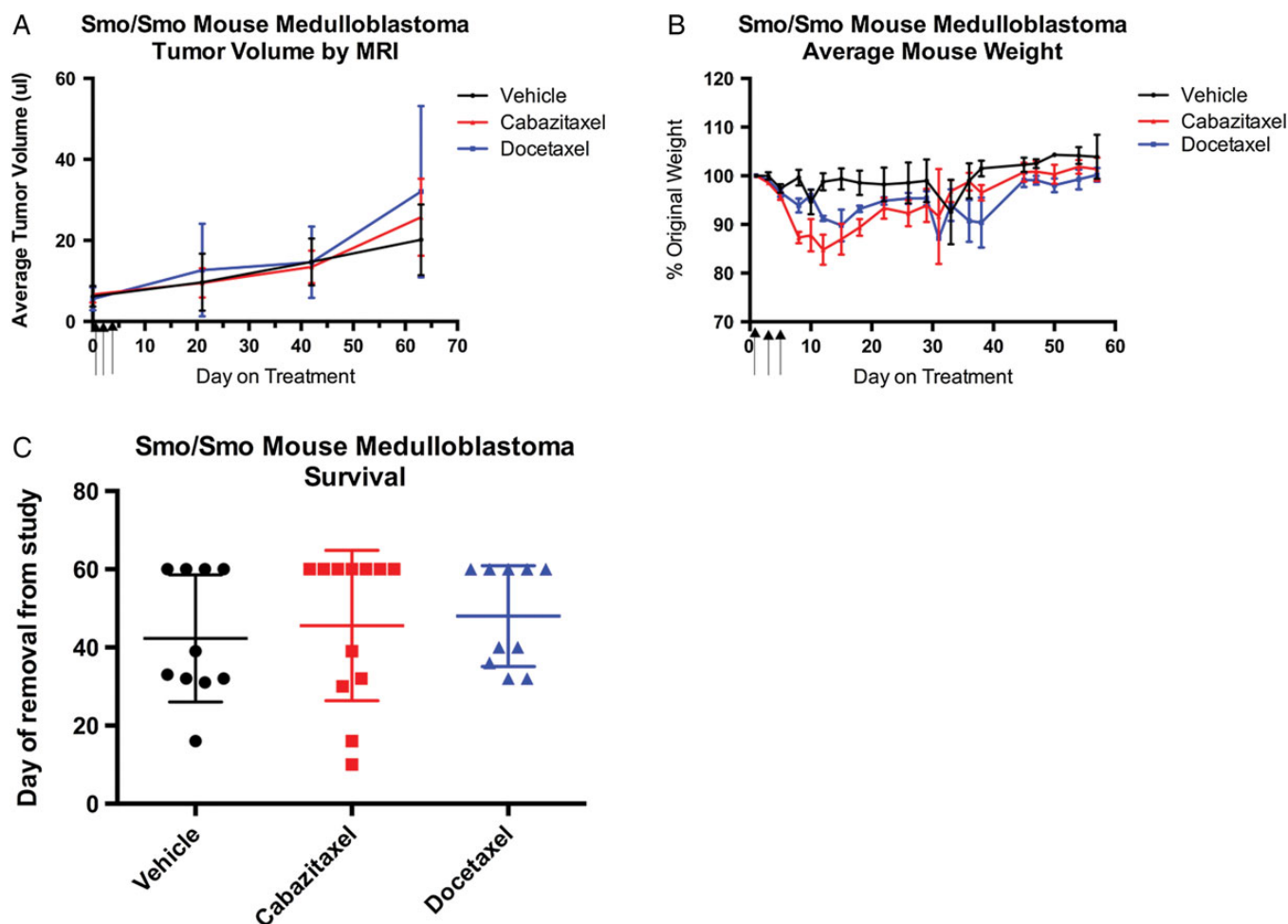


**Fig. 3.** Activity of cabazitaxel and docetaxel in hedgehog-driven Smo/Smo spontaneous mouse medulloblastoma. MRI was performed prior to initiation of treatment to determine tumor volume and BBB integrity. Mice with tumors between 4 mm<sup>2</sup> and 16 mm<sup>2</sup> that lacked gadolinium contrast staining in the tumor were randomly enrolled into treatment groups. Enrolled mice received i.p. injections of cabazitaxel or docetaxel (15 mg/kg) on days 1, 3, and 5. MRI was repeated 3, 5, and 9 weeks after study enrollment with gadolinium contrast staining being included at weeks 5 and 9. (A) Mean tumor volume for each treatment group  $\pm$  SEM. Tumor volume was calculated by 3-dimensional reconstruction of MR images. (B) Average mouse weight  $\pm$  SEM as a percentage of the starting weight for each dosing group. (C) Survival of mice (group average  $\pm$  SEM) from each treatment group.

mice with ATRT-310FH tumors was 14.5 days with vehicle (v), 22 days with docetaxel (d), and 34.1 days with cabazitaxel (c) treatment. Mean survival of the cabazitaxel group was significantly different from both the vehicle ( $P < .0001$ ) and docetaxel ( $P = .0025$ ) groups. Survival was not significantly different between the vehicle and docetaxel groups ( $P = .0833$ ) (Fig. 4C). Mice with the Med-211FH orthotopic tumors had a median survival of 15.11 (v), 17.33 (d), and 26.78 (c) days. Survival of the cabazitaxel-treated mice was significantly longer than the vehicle-treated group ( $P = .0028$ ) but was not significantly different from the docetaxel group ( $P = .0953$ ), nor was the docetaxel group significantly different from the vehicle-treated group ( $P > .9999$ ) (Fig. 4D). Median survival of the PNET-109FH tumor model was 10.33 (v), 20.78 (d), and 30.83 (c) days. Survival was improved for both the cabazitaxel- and docetaxel-treated groups compared with vehicle ( $P < .0001$ ). Additionally, survival of the cabazitaxel group was significantly longer than the docetaxel group ( $P < .0001$ ) (Fig. 4E).

## Discussion

The treatment of pediatric brain tumors is a delicate balance between aggressive elimination of cancer cells, for preserving the child's life, and protection of healthy neural tissue, for preserving the child's normal motor and cognitive function. The standard of care with the best possibility of long-term survival (tumor resection and craniospinal radiation) can result in crippling neural toxicity.<sup>4,10,24,25</sup> Additionally, there are some brain tumors that cannot be resected because of their location in the central nervous system, and radiation therapy is not recommended for children under aged 3 years.<sup>26,27</sup> The sought-after solution for pediatric neuro-oncology patients is a therapeutic that is able to penetrate into the brain and selectively kill cancer cells with minimal toxicity to normal neurons.

Taxane therapies have a history of effective treatment for adult solid tumors. Paclitaxel and docetaxel have been approved for the treatment of breast, ovarian, lung, esophageal,

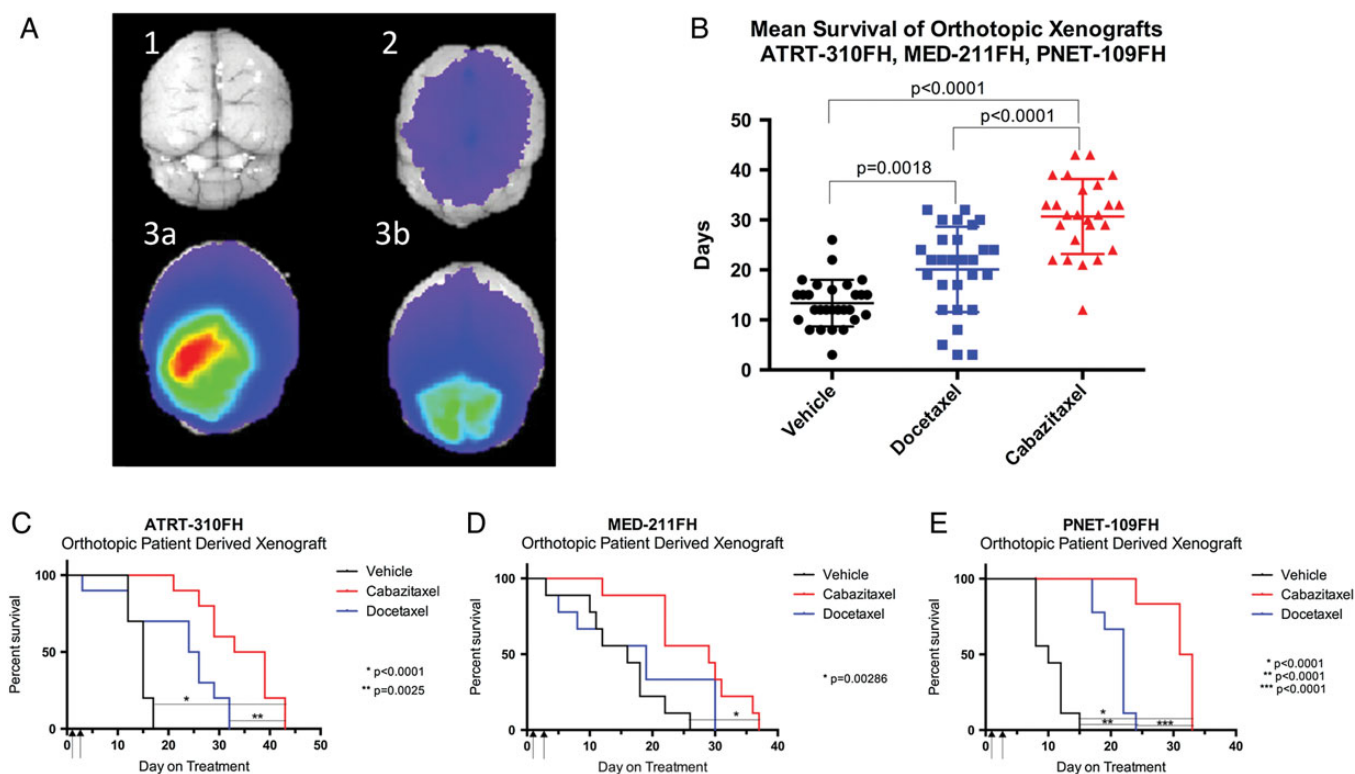


**Fig. 4.** Comparison of antitumor activity of cabazitaxel and docetaxel in orthotopic pediatric patient-derived xenografts. Patient-derived models of ATRT, medulloblastoma, and CNS-PNET were transplanted as orthotopic xenografts into the cerebrum (ATRT-310FH and PNET-109FH) or the cerebellum (MED-211FH) of male or female NOD:scid gamma mice. Either cabazitaxel or docetaxel was administered on days 1 and 3 by i.p. injection at 15 mg/kg. (A) To determine readiness of orthotopic xenografts for study enrollment, tumor burden was assessed in 2 randomly chosen mice. Mice received an i.v. injection of chlorotoxin-Cy5.5, and brains were imaged ex vivo in the near-infrared spectrum 3 hours after injection. Positive signal, indicating significant, but not symptomatic, tumor burden triggered study initiation. (A1) Nontumor-bearing, noninjected negative control brain. (A2) Nontumor-bearing, CTX-Cy5.5-injected negative control brain. (A3A and A3B) Representative, Med-211FH tumor-bearing, CTX-Cy5.5 injected brains ex vivo. (B) Combined mean survival of the ATRT-310FH, MED-211FH, and PNET-109FH orthotopic models. Mouse survival by treatment group in individual tumor models. (C) ATRT-310FH; (D) MED-211FH; and (E) PNET-109FH.

bladder, endometrial, cervical, prostate, stomach, and head and neck cancers.<sup>28,29</sup> Cabazitaxel is a taxane derivative selected for clinical development based on its broad spectrum of antitumor activity, not only on taxane-sensitive tumor models, but also on tumor models poorly or not sensitive to taxanes.<sup>19</sup> Cabazitaxel is approved in various countries and regions worldwide for the treatment of patients with metastatic hormone-refractory prostate cancer who are experiencing disease progression following docetaxel therapy. In contrast to docetaxel and paclitaxel, cabazitaxel is able to cross the BBB.<sup>13</sup> Furthermore, there is evidence that cabazitaxel not only crosses into the neuronal capillary endothelial cells but also accumulates in the brain parenchyma.<sup>13,18</sup> The potent antimitotic activity of taxanes with the ability to penetrate through the BBB makes cabazitaxel an attractive therapeutic strategy.

The results from this study show that cabazitaxel may be superior to docetaxel in its ability to inhibit tumor progression when treated systemically against patient-derived models of ATRT, medulloblastoma, and CNS-PNET. The flank xenograft models allow us to demonstrate that cabazitaxel inhibits tumor growth to an equal or greater extent than docetaxel, but these models lack the important biology of the BBB.

Evaluation of both therapeutics in orthotopic, patient-derived xenografts shows that cabazitaxel prolongs the survival of mice when compared with docetaxel.

The cellular mechanisms that result in greater growth inhibition in flank tumors and improved survival of orthotopic xenografts with cabazitaxel treatment are not explicitly known. Comparisons of cell cycle arrest, proliferation, and apoptosis in tumor cell lines in vitro report that cabazitaxel and docetaxel suppress proliferation, induce G2M arrest, and promote apoptosis to a similar degree in taxane-sensitive models.<sup>12,18,19,30-32</sup> In unpublished data from this study, a small subset of MED-211FH flank xenograft tumors were dosed once with cabazitaxel or docetaxel at 15 mg/kg and harvested 24 hours later. No difference in induction of markers for apoptosis (cleaved caspase3) or proliferation (Ki67) were observed between cabazitaxel and docetaxel. Cabazitaxel has shown superior inhibition of proliferation and induction of apoptosis in taxane-resistant tumor cell lines and xenograft models.<sup>12,13,18,19,29,31</sup> Though mechanisms of resistance to taxanes have not been fully elucidated, in cell lines, overexpression of ATP-binding transporters, particularly P-glycoprotein, and alteration of microtubule dynamics are the most common mechanisms of taxane resistance.<sup>33</sup> These results would suggest that

the more potent antitumor activity of cabazitaxel might be due to higher and more sustained drug exposure, when compared with docetaxel, because cabazitaxel has a greater lipophilicity than docetaxel. Further investigation is needed to determine if the higher lipophilicity of cabazitaxel does indeed result in greater drug exposure in flank tumors and across the BBB, resulting in more potent tumor inhibition.

We also used a hedgehog-driven genetic model of medulloblastoma, the Smo/Smo mouse. In this experiment, neither cabazitaxel nor docetaxel inhibited growth of in situ brain tumors. A dose response study in flank allograft tumors informed the 15 mg/kg dose regimen in the brain tumor study. 15 mg/kg given by i.p. injection on days 1, 3, and 5 is similar, though not identical, to other dosing regimen found to be efficacious against preclinical models of melanoma, sarcoma, glioblastoma, and colon, breast, pancreatic, prostate, lung, gastric, head and neck, and renal cancer.<sup>18,19</sup> The response of smo/smo medulloblastoma flank allograft tumors to cabazitaxel or docetaxel at 15 mg/kg was heterogeneous. While most tumors regressed in response to treatment, at least one tumor per treatment group continued to grow uninhibited. The heterogeneous response of flank tumor xenografts suggests that the therapeutic window in this model is narrow. In another preclinical therapeutic study using this medulloblastoma model, an upregulation in expression of Pgp in tumor homogenates was observed after daily treatment with smo inhibitor Saridegib for 6 weeks.<sup>34</sup> If a similar upregulation of Pgp were to occur in response to cabazitaxel treatment in this model, it is possible that a higher saturation threshold could be necessary to evade Pgp efflux from the endothelial capillaries. Further studies are needed to explore this possibility. Taken together, the heterogeneity of flank tumor response and the historic knowledge that this medulloblastoma model can upregulate expression of Pgp may suggest that the therapeutic window for cabazitaxel in the Smo/Smo model is narrow and that there may have been insufficient exposure to cabazitaxel in this model to effect tumor growth, even with the well-documented ability of cabazitaxel to cross the BBB.

Finding a treatment that has efficacy against orthotopic ATRT, medulloblastoma, and CNS-PNET patient-derived brain xenograft tumors is encouraging and endorses further investigation of cabazitaxel. CNS-PNET and ATRT in particular have poor long-term survival rates and typically occur in very young patients with developing brains vulnerable to radiation. No drug candidate has previously been brought into clinical trials based on preclinical activity against an ATRT tumor model. These data support the newly initiated phase 1 clinical trial of cabazitaxel in pediatric brain tumor patients (NCT01751308) and impart optimism that this therapeutic may enhance the quantity and quality of life for pediatric neuro-oncology patients.

## Funding

This work was sponsored by Sanofi Global Oncology Inc.; development of the PDX tumor models was supported by National Institutes of Health/National Cancer Institute grants [R01-CA112250, R01-CA135491]; Seattle Children's Brain Tumor Endowment; The Run of Hope.

## Acknowledgments

The authors would like to thank the patients and families who have contributed tissue for the patient-derived xenograft models. Thank you for the contributions of Kyle Pedro and Alex Brown, Comparative Medicine, and Experimental Histopathology at the Fred Hutchinson Cancer Research Center.

**Conflict of interest statement.** This work was sponsored by the Sanofi Oncology/Global Oncology Division. Authors Patricia Vrignaud and Dmitri Bobilev are employees of Sanofi and provided technical guidance for these experiments as members of the project steering committee.

## Unpublished papers cited

None.

## References

- Babcock MA, Kostova FV, Fountain J, et al. Tumors of the central nervous system: clinical aspects, molecular mechanisms, unanswered questions, and future research directions. *J Child Neurol.* 2013;23(10):1103–1121. doi:10.1177/0883073808321767.
- Mueller S, Chang S. Pediatric brain tumors: current treatment strategies and future therapeutic approaches. *Neurotherapeutics.* 2009;6(3):570–586. doi:10.1016/j.nurt.2009.04.006.
- Ginn KF, Gajjar A. Atypical teratoid rhabdoid tumor: current therapy and future directions. *Front Oncol.* 2012;2:114.
- Diller L, Chow EJ, Gurney JG, et al. Chronic disease in the Childhood Cancer Survivor Study cohort: a review of published findings. *J Clin Oncol.* 2009;27(14):2339–2355. doi:10.1200/JCO.2008.21.1953.
- Witt KA, Gillespie TJ, Huber JD, et al. Peptide drug modifications to enhance bioavailability and blood-brain barrier permeability. *Peptides.* 2001;22(12):2329–2343.
- Willis CL. Glia-induced reversible disruption of blood-brain barrier integrity and neuropathological response of the neurovascular unit. *Toxicol Pathol.* 2011;39(1):172–185.
- Daneman R. The blood-brain barrier in health and disease. *Ann Neurol.* 2012;72(5):648–672.
- Pardridge WM. The blood-brain barrier: bottleneck in brain drug development. *NeuroRx.* 2005;2(1):3–14.
- Alavijeh MS, Chishty M, Qaiser MZ, et al. Drug metabolism and pharmacokinetics, the blood-brain barrier, and central nervous system drug discovery. *NeuroRx.* 2005;2(4):554–571.
- Ellenberg L, Liu Q, Gioia G, et al. Neurocognitive Status in Long-Term Survivors of Childhood CNS Malignancies: A Report from the Childhood Cancer Survivor. *Neuropsychology.* 2009;23(6):705–717.
- Neuwelt EA. Mechanisms of Disease: The Blood-Brain Barrier. *Neurosurgery.* 2004;54(1):131–142.
- Bouchet BP, Galmarini CM. Cabazitaxel, a new taxane with favorable properties. *Drugs Today (Barc).* 2010;46:735–742.
- Cisternino S, Bourasset F, Archimbaud Y, et al. Nonlinear accumulation in the brain of the new taxoid TXD258 following saturation of P-glycoprotein at the blood-brain barrier in mice and rats. *Br J Pharmacol.* 2003;138(7):1367–1375.



14. Blaney SM, Seibel NL, O'Brien M, et al. Phase I trial of docetaxel administered as a 1-hour infusion in children with refractory solid tumors: a collaborative pediatric branch, National Cancer Institute and Children's Cancer Group trial. *J Clin Oncol*. 1997; 15(4):1538–1543.
15. Zwerdling T, Krailo M, Monteleone P, et al. Phase II investigation of docetaxel in pediatric patients with recurrent solid tumors: a report from the Children's Oncology Group. *Cancer*. 2006;106(8): 1821–1828.
16. Hurwitz CA, Relling MV, Weitman SD, et al. Phase I trial of paclitaxel in children with refractory solid tumors: a Pediatric Oncology Group Study. *J Clin Oncol*. 1993;11(12):2324–2329.
17. Tsao C-K, Seng S, Oh WK, et al. Clinical development of cabazitaxel for the treatment of castration-resistant prostate cancer. *Clin Med Insights Oncol*. 2011;5:163–169.
18. Sémiond D, Sidhu SS, Bissery M-C, et al. Can taxanes provide benefit in patients with CNS tumors and in pediatric patients with tumors? An update on the preclinical development of cabazitaxel. *Cancer Chemother Pharmacol*. 2013;72(3):515–528.
19. Vrignaud P, Sémiond D, Lejeune P, et al. Preclinical antitumor activity of cabazitaxel, a semisynthetic taxane active in taxane-resistant tumor. *Clin Cancer Res*. 2013;19(11):2973–2983.
20. Hatton BA, Villavicencio EH, Tsuchiya KD, et al. The Smo/Smo model: hedgehog-induced medulloblastoma with 90% incidence and leptomeningeal spread. *Cancer Res*. 2008;68(6): 1768–1776.
21. Hallahan AR, Pritchard JI, Hansen S, et al. The smoa1 mouse model reveals that notch signaling is critical for the growth and survival of sonic hedgehog-induced medulloblastomas. *Cancer Res*. 2004;64:7794–7800.
22. Veiseh M, Gabikian P, Bahrami S-B, et al. Tumor paint: a chlorotoxin:cy5.5 bioconjugate for intraoperative visualization of cancer foci. *Cancer Res*. 2007;67(14):6882–6888.
23. Stroud MR, Hansen SJ, Olson JM. In vivo bio-imaging using chlorotoxin-based conjugates. *Curr Pharm Des*. 2011;17(38): 4362–4371.
24. Smith MA, Seibel NL, Altekruze SF, et al. Outcomes for children and adolescents with cancer: challenges for the twenty-first century. *J Clin Oncol*. 2010;28:2625–2634.
25. Robison LL, Armstrong GT, Boice JD, et al. The Childhood Cancer Survivor Study: a National Cancer Institute-supported resource for outcome and intervention research. *J Clin Oncol*. 2009; 27(14):2308–2318.
26. Bishop AJ, McDonald MW, Chang AL, et al. Infant brain tumors: incidence, survival, and the role of radiation based on Surveillance, Epidemiology, and End Results (SEER) Data. *Int J Radiat Oncol Biol Phys*. 2012;82:341–347.
27. Gottardo NG, Gajjar A. Chemotherapy for malignant brain tumors in childhood. *J Child Neurol*. 2008;23(10):1149–1159.
28. Villanueva C, Awada A, Campone M, et al. A multicentre dose-escalating study of cabazitaxel (XRP6258) in combination with capecitabine in patients with metastatic breast cancer progressing after anthracycline and taxane treatment: a phase I/II study. *Eur J Cancer*. 2011;47(7):1037–1045.
29. Galsky MD, Dritselis A, Kirkpatrick P, et al. Cabazitaxel. *Nat Rev Drug Discov*. 2010;9(9):677–678.
30. Yoo GH, Kafri Z, Ensley JF, et al. XRP6258-Induced gene expression patterns in head and neck cancer carcinoma. *Laryngoscope*. 2010; 120:1114–1119.
31. Villanueva C, Bazan F, Kim S, et al. Cabazitaxel: a novel microtubule inhibitor. *Drugs*. 2011;71:1251–1258.
32. Ganansia-Leymarie V, Bischoff P, Bergerat J-P, et al. Signal transduction pathways of taxanes-induced apoptosis. *Curr Med Chem Anticancer Agents*. 2003;3:291–306.
33. Greenberger LM, Sampath D. Resistance to taxanes. In: Teicher BA, ed. *Cancer Drug Resistance*. Totowa, NJ: Humana Press;2006; 329–358.
34. Lee MJ, Hatton BA, Villavicencio EH, et al. Hedgehog pathway inhibitor saridegib (IPI-926) increases lifespan in a mouse medulloblastoma model. *Proc Natl Acad Sci USA*. 2012;109(20): 7859–7864.